Available online at www.sciencedirect.com
SCIENCE DIRECT®
Bioorganic & Medicinal Chemistry Letters 14 (2004) 4825–4829
Bioorganic & Medicinal Chemistry Letters

Computational comparison of microtubule-stabilising agents laulimalide and peloruside with taxol and colchicine

Oriol Pineda,[a] Jaume Farràs,[a] Laura Maccari,[b] Fabrizio Manetti,[b] Maurizio Botta[b] and Jaume Vilarrasa[a,*]

[a]*Departament de Química Orgànica, Facultat de Química, Universitat de Barcelona, 08028 Barcelona, Catalonia, Spain, EU*
[b]*Dipartimento Farmaco Chimico Tecnologico, Università degli Studi di Siena, 53100 Siena, Italy, EU*

Received 4 May 2004; revised 5 July 2004; accepted 23 July 2004
Available online 13 August 2004

Abstract—Microtubule-stabilising agents laulimalide and peloruside have been compared with tubulin-interacting drugs paclitaxel and colchicine by different computational approaches. Docking and QSAR-based programs point to a favourable interaction with the β tubulin paclitaxel binding site, although an additional, preferred binding site has been found at the α subunit of tubulin. All together provides a plausible rationalisation of the singular binding features of these microtubule stabilisers and paves the way for future structural studies.

Taxol® (paclitaxel, **1**) is an important antimitotic agent broadly used for the treatment of ovarian, breast and lung carcinomas;[1] it causes cell cycle arrest by interfering in the G2/M phase. Since the discovery of its microtubule-stabilising mechanism of action,[2] other drugs have been found to exert analogous effects. This is the case of epothilones,[3] sarcodictyins,[2] discodermolide,[4] laulimalide (**2**),[5] peloruside (**3**)[6] and many others.[2] These compounds are generically called microtubule-stabilising agents (MSA).

It is widely accepted that MSA interact at the β tubulin paclitaxel binding site (tax site), as most have been determined to compete with **1**.[2] However: (i) some of them are known to be active against cell lines resistant to others;[7] (ii) synergistic effects have been found between **1** and discodermolide;[4a] (iii) it has been shown that microtubules containing near-molar quantities of **1** and **2** can be formed;[8] (iv) the binding site of a few MSA has not been established yet (this is the case of **3**); (v) independent photoaffinity labelling experiments with azide-containing derivatives of **1** point to diverse binding targets on tubulin.[9] With relatively close 3-D shapes (Fig. 1),[10,11] the differences in the biological behaviour of these MSA are likely to be due to the obvious diversity of molecular structures (functional groups, side chains, etc.).

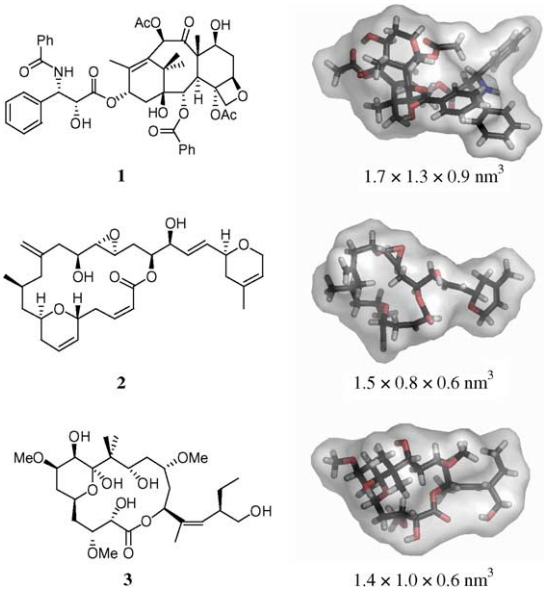

Figure 1. 3-D representations[10,11] of MSA paclitaxel (**1**),[11b] laulimalide (**2**) and peloruside (**3**).

Keywords: Anti-cancer drugs; Modelling; Docking; Laulimalide; Peloruside.
* Corresponding author. Tel.: +34-934021258; fax: +34-933397878; e-mail: jvilarrasa@ub.edu

0960-894X/$ - see front matter © 2004 Elsevier Ltd. All rights reserved.
doi:10.1016/j.bmcl.2004.07.053

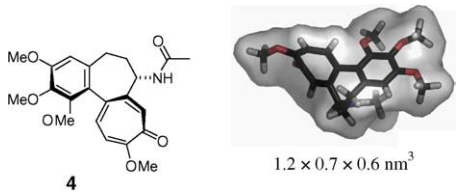

Figure 2. 3-D representation[10,11] of MDA colchicine (**4**).

On the other hand, there are drug families that have been found to interact with microtubules in a different way. The microtubule-destabilising agent (MDA) colchicine (**4**, Fig. 2) is an example of them. This compound and its congeners have been determined to interact at the so-called colchicine binding site (colchi site), although additional binding has been described to take place near the tax site.[12]

We report here computational approaches aimed at rationalising some of these interesting facts. We have chosen **1** and **4** as well-known reference compounds to investigate the less known tubulin-binding features of MSA **2** and **3**.

Docking approaches: First, we focused our work on finding out the binding modes of **1**–**4** by means of a blind-docking procedure.[13] The well-established tubulin structure determined by Nogales et al.[14] was used as the target of our docking simulations. Among the several docking programs available, we chose AutoDock 3.05[15] to find the binding modes of the studied compounds,[16] and GOLD 2.1[17] to score the resulting complexes.[18] The reliability of the approach was evaluated by reproducing the complex of **1** with this tubulin structure. The predicted complex (the highly scored one) gave a RMSD of 0.79 Å with regard to the experimental one.[14b,19] Docking of **4** was also consistent with the experimental facts, since it predicted **4** to bind mainly at the colchi site, with a lower-scored interaction with the tax site. The tax and colchi sites are shown in Figure 3.

In the first round of docking simulations, compounds **2** and **3** were predicted to bind mainly at the tax site.[20]

In addition, the predicted arrangement of **2** into the tax site explains the activity retention of this compound against cell lines resistant to **1** or to epothilone B.[8] Those amino acids involved in the mutations associated to these cell lines do not interact with **2** in our AutoDock-predicted binding mode (Fig. 4).

Even though this finding supports the binding of **2** to the tax site, it provides no explanation for the formation of microtubules containing equimolar amounts of **1** and **2**.[8] In a second round of simulations, this goal was pursued, as follows.

We searched for an additional binding site over a mobile region of α tubulin, the B9–B10 loop extension.[21] This loop has a special relevance, since it covers the region of α tubulin related with the tax site at β tubulin.[11b] The conformation of this B9–B10 loop extension was explored with MacroModel,[11a] by manual search and molecular dynamics simulations (MD). Both approaches gave rise to a lower energy local minimum by rotation of the mentioned loop (Fig. 5), disclosing a new cavity fairly similar to the tax site.

Docking simulations were repeated with the B9–B10 loop extension open. This new binding site (henceforward the B9–B10 site) was predicted to be accessible for **2**–**4**, but not for **1** (which may be due to its larger size, see Fig. 1). Location of this new binding site at the α subunit of tubulin is shown in Figure 6.

Scoring of the complexes of **1**–**3** with the B9–B10 site was then performed[18] and compared with the respective complexes with the tax site (Table 1). Reference compound **1** was correctly predicted to bind the tax site. Compound **2** was predicted by the two scoring functions to have a preference for the B9–B10 site. Regarding compound **3**, AutoDock predicted a certain preference for the B9–B10 site, although GoldScore predicted a

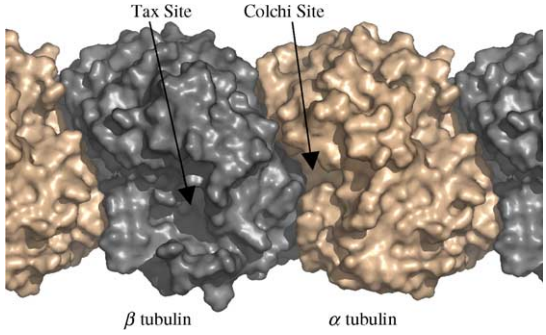

Figure 3. The tax site and the colchi site of tubulin.[10]

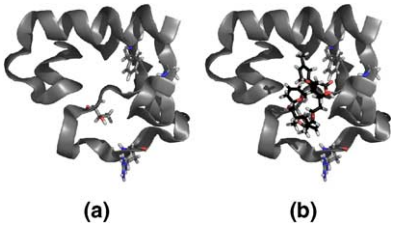

Figure 4. (a) The tax site, depicting the amino acids mutated in cell lines PTX10 (Phe270Val), PTX22 (Ala364Thr), A8 (Thr274Ile) and B10 (Arg282Gln).[8] (b) Compound **2** docked into the tax site.

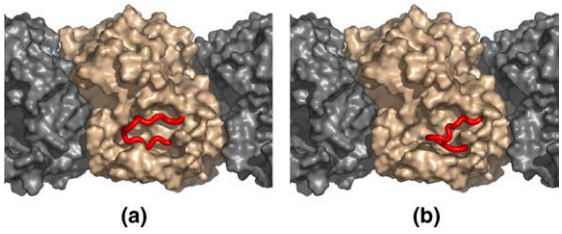

Figure 5. The B9–B10 loop extension of α tubulin depicted in red. (a) Original conformation and (b) that one disclosing a new cavity.

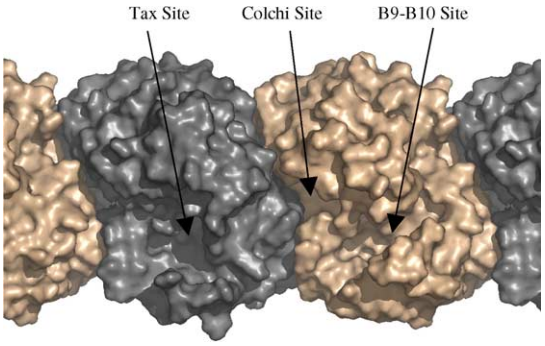

Figure 6. The MD-predicted B9–B10 site, in relation to the tax site and the colchi site of tubulin.

Table 1. Scoring of the complexes of **1**–**3** at the B9–B10 site, referred to that of complexes at the tax site, indicated within parentheses

	AutoDock[a]	GoldScore[b]
1	−5.8 (−8.1)	21 (41)
2	−11.4 (−10.2)	59 (50)
3	−5.6 (−4.8)	13 (18)

[a] Values in kcal/mol.
[b] Better scoring corresponds to higher figures.

trend for the tax site, which may indicate that the strength of the interaction of **3** with both sites is essentially equivalent. As expected, reference compound **4** was correctly predicted to bind the colchi site (data not shown).

To summarise, the available experimental data are qualitatively described by the main results from these docking simulations: (i) compound **1** is predicted to bind at the tax site;[9] (ii) compound **4** is predicted to bind mainly at the colchi site, although a weaker interaction is also observed with the tax site;[12] (iii) compound **2** is predicted not only to bind the tax site but also to an alternative, preferred one.[8] Thus, a plausible explanation for the formation of microtubules containing equimolar amounts of **1** and **2**[8] is provided, as **2** may interact at the B9–B10 site of tubulin when the tax site is occupied by **1**.

Nevertheless, these simulations and the experiments with mutant cells still point to the binding of **2** and **3** to the tax site, even though not predominantly. A quantitative treatment would be required to determine the strength of this interaction.

QSAR approaches: Among the tax site receptor models reported to date,[22] we have chosen the more versatile one,[22a] that one able to better accommodate different families of compounds. This 3D-QSAR model consists of a 21 amino acid box surrounding a set of MSA (including **1**, epothilones, sarcodictyins and several derivatives of them). We have used this model to predict ΔG_{bind} for **2** and **3**. Calculations, performed with PrGen 2.1[23] and AutoDock, predict a strong interaction of both compounds with the tax site. Complexes of **2** and **3** with the receptor model and the main interactions are shown in Figure 7.

To overcome the assumptions made on the construction of the 3D-QSAR receptor model—selection of amino acids, alignment of ligands, etc.—we built up, by means of Quasar 3.0,[24] a 5D-QSAR model of the tax site.[25] Again, compounds **2** and **3** were predicted to strongly bind the tax site.

Predictions performed with the two receptor models (Table 2) show a good agreement between experimental

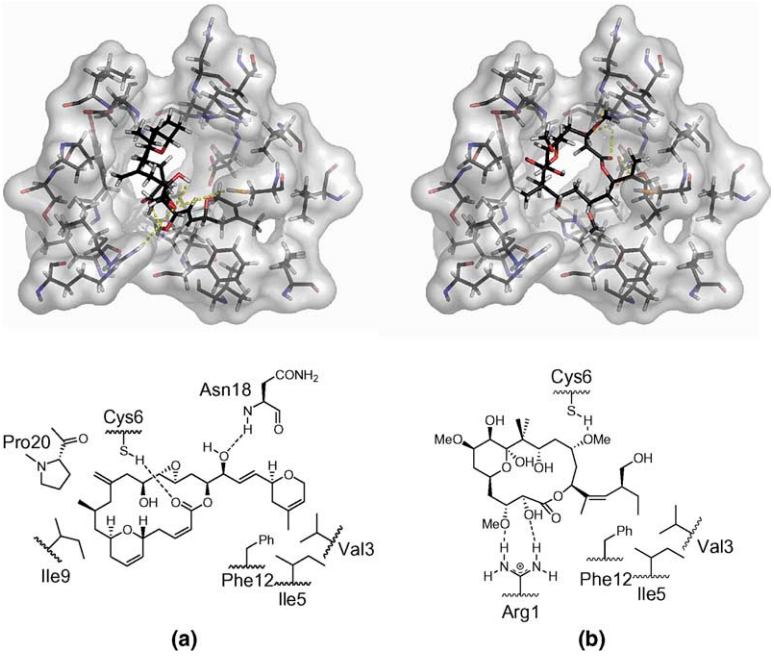

Figure 7. Complexes and main interactions of **2** (a) and **3** (b) with the tax site receptor model.[22a]

Table 2. Predicted ΔG_{bind} compared with the experimental values[a]

	Experimental ΔG_{bind}	PrGen-predicted ΔG_{bind}	AutoDock-predicted ΔG_{bind}	Quasar-predicted ΔG_{bind}
1	−6.5	−6.6	−6.8	−6.6
2	−6.0	−5.8	−8.7	−5.9
3	—	−6.5	−5.1	−6.7
ent-**3**[b]	—	−5.8	−5.0	−4.5

[a] All values in kcal/mol.

[b] We have also calculated the affinity of this enantiomer, since its total synthesis has been reported.[6c]

and predicted ΔG_{bind} for **1** (included into the training sets) and **2** (included into the test sets). Regarding **3**, a fair agreement was found between PrGen-, AutoDock- and Quasar-predicted ΔG_{bind} values (no tubulin binding constants have been reported for **3** to our knowledge). The interaction of **2** and **3** with the tax site is predicted to be in the range of strong MSA, showing therefore the virtual capability of **2** and **3** to bind to the tax site.

Concluding remarks: In silico studies, which we have shown to be consistent with the experimental findings, provide an explanation for the surprising interaction of **2** with tubulin: formation of microtubules containing equimolar amounts of **1** and **2** can be qualitatively rationalised by the simulations performed, since the proposed laulimalide binding site has been predicted to be located at α tubulin, under the B9–B10 loop extension. Lack of competition of **2** for the tax site (when **1** is bound to it) is accounted for qualitatively, but the predicted binding affinity difference is lower than expected.

In addition, simulations predict the behaviour of **3** to be closely related to that of **2**. Therefore, binding features of **2** should be also observed for **3**. Moreover, interaction of **2** and **3** with the tax site has been found to be still favourable, in the range of potent MSA, indicating the ability of these compounds to bind secondarily the tax site and to act as paclitaxel-like MSA.

In summary, the results here presented explain singular binding features of these MSA and paves the way for future structural studies.

Acknowledgements

Financial support to both the Barcelona and Siena groups from the Research Directorate General of the EU (Network HPRN-CT-2000-018) is acknowledged. Thanks are also due to the Ministerio de Ciencia y Tecnología (PM98-1272, SAF02-02728) and DURSI, Generalitat de Catalunya (2001SGR 051).

Supplementary data

Supplementary data associated with this article can be found, in the online version, at doi:10.1016/j.bmcl.2004.07.053.

References and notes

1. (a) McGuire, W. P.; Rowinsky, E. K.; Rosenshein, N. B.; Grumbine, F. C.; Ettinger, D. S.; Armstrong, D. K.; Donehower, R. C. *Ann. Intern. Med.* **1989**, *111*, 273–279; (b) Holmes, F. A.; Walters, R. S.; Theriault, R. L.; Forman, A. D.; Newton, L. K.; Raber, M. N.; Buzdar, A. U.; Frye, D. K.; Hortobagyo, G. N. *J. Natl. Cancer Inst.* **1991**, *83*, 1797–1805.
2. For excellent reviews on the 'α tubulin + β tubulin heterodimer/protofilament/microtubule' equilibria and, in general, on microtubule-stabilising or destabilising molecules, see: (a) Hadfield, J. A.; Ducki, S.; Hirst, N.; McGown, A. T. *Progr. Cell Cycle Res.* **2003**, *5*, 309–325; (b) Jiménez-Barbero, J.; Amat-Guerri, F.; Snyder, J. P. *Curr. Med. Chem.—Anti-Cancer Agents* **2002**, *2*, 91–122; (c) Nogales, E. *Ann. Rev. Biophys. Biomol. Struct.* **2001**, *30*, 397–420; (d) He, L.; Orr, G. A.; Horwitz, S. B. *Drug Discov. Today* **2001**, *6*, 1153–1164; (e) Altmann, K.-H. *Curr. Opin. Chem. Biol.* **2001**, *5*, 424–431; (f) Amos, L. A.; Löwe, J. *Chem. Biol.* **1999**, *6*, 65–69.
3. For leading reviews on epothilones, see: (a) Nicolaou, K. C.; Roschangar, F.; Vourloumis, D. *Angew. Chem., Int. Ed.* **1998**, *37*, 2014–2045; (b) Stachel, S. J.; Biswas, K.; Danishefsky, S. J. *Curr. Pharm. Design.* **2001**, *7*, 1277–1290; For very recent works, see: (c) Chou, T.-C.; Dong, H.; Rivkin, A.; Yoshimura, F.; Gabarda, A. E.; Cho, Y. S.; Tong, W. P.; Danishefsky, S. J. *Angew. Chem., Int. Ed.* **2003**, *42*, 4762–4767, and references cited therein; (d) For NMR studies on tubulin–epothilone complexes: Carlomagno, T.; Blommers, M. J. J.; Meiler, J.; Jahnke, W.; Schupp, T.; Petersen, F.; Schinzer, D.; Altmann K.-H.; Griesinger, C. *Angew. Chem., Int. Ed.* **2003**, *42*, 2511–2515; (e) Carlomagno, T.; Sánchez, V. M.; Blommers, M. J. J.; Griesinger, C. *Angew. Chem., Int. Ed.* **2003**, *42*, 2515–2517.
4. (a) Martello, L. A.; McDaid, H. M.; Regl, D. L.; Yang, C. P. H.; Meng, D.; Pettus, T. R. R.; Kaufman, M. D.; Arimoto, H.; Danishefsky, S. J.; Smith, A. B. *Clin. Canc. Res.* **2000**, *6*, 1978–1987; For modeling and/or conformational studies on discodermolide, see: (b) Martello, L. A.; LaMarche, M. J.; He, L.; Beauchamp, T. J.; Smith, A. B.; Horwitz, S. B. *Chem. Biol.* **2001**, *8*, 843–855; (c) Smith, A. B.; LaMarche, M. J.; Falcone-Hindley, M. *Org. Lett.* **2001**, *3*, 695–698; (d) Monteagudo, E.; Cicero, D. O.; Cornett, B.; Myles, D. C.; Snyder, J. P. *J. Am. Chem. Soc.* **2001**, *123*, 6929–6930; For total syntheses, see: (e) Smith, A. B.; Freeze, B. S.; Brouard, I.; Hirose, T. *Org. Lett.* **2003**, *5*, 4405–4408, and Ref. 6 cited therein.
5. For leading references on **3**, see: (a) Wender, P. A.; Hegde, S. G.; Hubbard, R. D.; Zhang, L.; Mooberry, S. L. *Org. Lett.* **2003**, *5*, 3507–3509; (b) Mooberry, S. L.; Tien, G.; Hernandez, A. H.; Plubrukarn, A.; Davidson, B. S. *Cancer Res.* **1999**, *59*, 653–660; (c) Quiñoà, E.; Kakou, Y.; Crews, P. *J. Org. Chem.* **1988**, *53*, 3642–3644; (d) Corely, D. G.; Herb, R.; Moore, R. E.; Scheuer, P. J. *J. Org. Chem.* **1988**, *53*, 3644–3646; (e) For total syntheses of **3**, see the following reviews: Crimmins, M. T. *Curr. Opin. Drug Discov. Devel.* **2002**, *5*, 944–959; (f) Mulzer, J.; Ölher, E. *Chem. Rev.* **2003**, *103*, 3753–3786.
6. For leading references on **4**, see: (a) Hood, K. A.; West, L. M.; Rouwé, B.; Northcote, P. T.; Berridge, M. V.; Wakefield, S. J.; Miller, J. H. *Cancer Res.* **2002**, *62*, 3356–3360; (b) West, L. M.; Northcote, P. T. *J. Org. Chem.* **2000**, *65*, 445–449; (c) For a total synthesis of the enantiomer of the natural product, see: Liao, X.; Wu, Y.; De Brabander, J. K. *Angew. Chem., Int. Ed.* **2003**, *42*, 1648–1652.

7. (a) Giannakakou, P.; Sackett, D. L.; Kang, Y.-K.; Zhan, Z.; Buters, J. T. M.; Fojo, T.; Poruchynsky, M. S. *J. Biol. Chem.* **1997**, *272*, 17118–17125; (b) Giannakakou, P.; Gussio, R.; Nogales, E.; Downing, K. H.; Zaharevitz, D.; Bollbuck, B.; Poy, G.; Sackett, D.; Nicolaou, K. C.; Fojo, T. *Proc. Natl. Acad. Sci. U.S.A.* **2000**, *97*, 2904–2909.
8. Pryor, D. E.; O'Brate, A.; Bilcer, G.; Díaz, J. F.; Wang, Y.; Kabaki, M.; Jung, M. K.; Andreu, J. M.; Ghosh, A. K.; Giannakakou, P.; Hamel, E. *Biochemistry* **2002**, *41*, 9109–9115.
9. For experiments where derivatives of **1** bind at β tubulin see: (a) Rao, S.; He, L.; Chakravarty, S.; Ojima, I.; Orr, G. A.; Horwitz, S. B. *J. Biol. Chem.* **1999**, *269*, 37990–37994, and references cited therein; (b) For experiments where derivatives of **1** bind at α and β tubulin see: Loeb, C.; Combeau, C.; Ehret-Sabatier, L.; Breton-Gilet, A.; Faucher, D.; Rousseau, B.; Commerçon, A. F.; Goeldner, M. *Biochemistry* **1997**, *33*, 3820–3825, and references cited therein.
10. Surface representations and approximate sizes of the 'boxes' that could encapsulate **1**–**4** have been obtained with PyMol. See: DeLano, W. L. The PyMol Molecular Graphics System, DeLano Scientific LLC, San Carlos, CA, USA (http://www.pymol.org).
11. We have obtained the 3-D structures of **2**–**4** by 10,000-step Monte Carlo conformational searches with MacroModel 7.2 (AMBER*/H_2O/GBSA): (a) Mohamadi, F.; Richards, N. G. J.; Guida, W. C.; Liskamp, R.; Lipton, M.; Caufield, C.; Chang, G.; Hendrickson, T.; Still, W. C. *J. Comput. Chem.* **1990**, *11*, 440–467; For a discussion on the bioactive conformation of **1**, see: (b) Snyder, J. P.; Nettles, J. H.; Cornett, B.; Downing, K. H.; Nogales, E. *Proc. Nat. Acad. Sci. U.S.A.* **2001**, *98*, 5312–5316.
12. Bai, R.; Covell, D. G.; Pei, X.-F.; Ewell, J. B.; Nguyen, N. Y.; Brossi, A.; Hamel, E. *J. Biol. Chem.* **2000**, *275*, 40443–40452; Chaudhuri, A. R.; Seetharamalu, P.; Schwarz, P. M.; Hausherr, F. H.; Ludueña, R. F. *J. Mol. Biol.* **2000**, *303*, 679–692.
13. Hetenyi, C.; VanDerSpoel, D. *Protein Sci.* **2002**, *11*, 1729–1737.
14. (a) Nogales, E.; Wolf, S. G.; Downing, K. H. *Nature* **1998**, *391*, 199–203; (b) Lowe, J.; Li, H.; Downing, K. H.; Nogales, E. *J. Mol. Biol.* **2001**, *313*, 1045–1057; (c) The structure here described has been demonstrated to fairly match with microtubules stabilised with **1**: Li, H.; DeRosier, D. J.; Nicholson, W. V.; Nogales, E.; Downing, K. H. *Structure* **2002**, *10*, 1317–1328.
15. Morris, G. M.; Goodsell, D. S.; Halliday, R. S.; Huey, R.; Hart, W. E.; Belew, R. K.; Olson, A. J. *J. Comput. Chem.* **1998**, *19*, 1639–1662.
16. Mai, A.; Massa, S.; Ragno, R.; Cerbara, I.; Jesacher, F.; Loidl, P.; Brosch, G. *J. Med. Chem.* **2003**, *46*, 512–524.
17. Jones, G.; Willett, P.; Glen, R. C.; Leach, A. R.; Taylor, R. *J. Mol. Biol.* **1997**, *267*, 727–748.
18. Docking simulations were performed with the structure reported in Ref. 14b. Only that surface relative to the lumen of the microtubule was considered (including the tax site and the colchi site) where stabilisation and destabilisation effect take place. Compound **1** was removed from the structure, while GDP and GTP were leaved untouched. Lamarckian genetic algorithm (LGA), 100 individuals, 5000 generations, 10^{10} energy evaluations, 50 LGA runs and a grid spacing of 0.75 Å were used with AutoDock to find the binding modes. Scoring of the different tubulin–drug complexes was performed with AutoDock (with a grid spacing of 0.30 Å) and GoldScore scoring functions.
19. In agreement with the experimental facts (Ref. 9b), lower-scored binding was also found to take place for **1** at the α subunit of tubulin, near amino acids 281–304.
20. Lower-scored binding was also found to take place for **2** and **3** with the colchi site, which, in fact, is reasonable, given that even **4** has been found to interact with the tax site (Ref. 13). Therefore, some reciprocity is likely to be observed between the two sites for the suitable compounds.
21. This region is characterised by a poor density in the electron crystallography model, meaning that its position is not firmly fixed. Therefore, it is a potential binding site for compounds capable of shifting its conformation. Other regions with similar mobility are present in tubulin, but only this one is facing the lumen of the microtubule, where stabilisation and destabilisation effects have been described to take place.
22. (a) Wang, M.; Xia, X.; Kim, Y.; Hwang, D.; Jansen, J. M.; Botta, M.; Liotta, D. C.; Snyder, J. P. *Org. Lett.* **1999**, *1*, 43–46; (b) Manetti, F.; Forli, S.; Maccari, L.; Corelli, F.; Botta, M. *Farmaco* **2003**, *58*, 357–361; (c) Maccari, L.; Manetti, F.; Corelli, F.; Botta, M. *Farmaco* **2003**, *58*, 659–668; For pharmacophore models of the tax site, see: (d) He, L.; Jagtap, P. G.; Kingston, D. G. I.; Shen, H.-J.; Orr, G. A.; Horwitz, S. B. *Biochemistry* **2000**, *39*, 3972–3978; (e) Ojima, I.; Chakravarty, S.; Inoue, T.; Lin, S.; He, L.; Horwitz, S. B.; Kuduk, S. D.; Danishefsky, S. J. *Proc. Nat. Acad. Sci. U.S.A.* **1999**, *96*, 4256–4261.
23. (a) Vedani, A.; Zbinden, P.; Snyder, J. P.; Greenidge, P. A. *J. Am. Chem. Soc.* **1995**, *117*, 4987–4994; (b) Zbinden, P.; Dobler, M.; Folkers, G.; Vedani, A. *Quant. Struct.—Act. Relat.* **1998**, *17*, 122–130.
24. Vedani, A.; Dobler, M. *J. Med. Chem.* **2002**, *45*, 2139–2149, Quasar 3.0 is a 5D-QSAR program that assumes no knowledge of the real receptor. The 4th D stands for multi-conformational and multi-tautomeric capabilities, and the 5th D stands for the induced fit of the model towards the training set.
25. This preliminary model was generated as follows: 250 randomly generated models were allowed to evolve by means of a Genetic Algorithm, using $q^2 = 0.950$ and RMS = 0.236 Å as ending criteria. The training set was composed by the MSA from Ref. 22a. Compounds **2** and **3** were entered in the test set.